Geoenvironmental Disasters

RESEARCH Open Access

Modelling terrain erosion susceptibility of logged and regenerated forested region in northern Borneo through the Analytical Hierarchy Process (AHP) and GIS techniques

H. Vijith* and D. Dodge-Wan

Abstract

This research examines the susceptibility of logged and regenerated forest region to erosion through the application of the analytical hierarchy process (AHP) and geographical information systems (GIS). In order to estimate terrain erosion susceptibility, ten geo-environmental variables were taken into account as possible factors relevant to terrain erosion. They are slope, aspect, relative relief, slope length and steepness (LS) factor, curvature, landforms, topographic wetness index (TWI), stream power index (SPI), stream head density, and land use/land cover. Pairwise comparison matrixes were generated to derive the weightages and ratings of each variable and their classes. These were integrated to generate the terrain erosion susceptibility index (TESI) map. Among the variables used in the analysis the land use/land cover, slope, SPI, stream head density, and LS factor were shown to have high contribution towards terrain erosion susceptibility. The areas with a concave slopes > 25° and high relative relief, LS factor, TWI, and stream head densities were found to be more susceptible to erosion such as gullying or landslides. The conversion of TESI into terrain erosion susceptibility zonation (TESZ) map shown that 25% of the total area is highly susceptible to erosion. Among this, 10% of the area possesses a very high vulnerability to landslides and gullying or soil slips and these areas coincide with logging roads and skidder trails. Linear regression analysis between TESI and TESZ with spatial distribution of mean annual rainfall in the region does not show any significant relationships ($p > 0.10$). However, high rainfall triggers rapid downstream movement of unsupported slopes in the region. The terrain erosion susceptibility zonation map expresses the realistic condition of logged terrain matching with field observations in the area in terms of erosion. The results can serve as basic data for future development programs in the region, in any projects where the terrain susceptibility is critical by planning infrastructure to avoid high risk zones.

Keywords: Geo-environmental variable, Terrain susceptibility, AHP, GIS, Borneo

* Correspondence: vijithh@gmail.com
Department of Applied Geology, Faculty of Engineering and Science, Curtin University Malaysia, CDT 250, 98009 Miri, Sarawak, Malaysia

Introduction

Erosion, either as soil loss or landslides, is the natural denudation process or a stage of geomorphic evolution of terrain which is responsible for generating different topographical features (Thornbury 1969). The natural erosional or denudational process will take place at given rate and any recent changes in the normal rate of erosion may reflect changes in the equilibrium condition of the terrain due to anthropogenic causes. Erosion and allied mass wasting problems are common in hilly areas, but their severity will vary depending on the geo-environmental factors involved. Steep sloping, highly elevated rugged terrain may be fragile in terms of geological, vegetation, and climatic factors making it more vulnerable to erosion, which may be aggravated by human induced developmental activities (Fadul et al. 1999). The fragility of such terrains can be termed as susceptibility to erosion. Assessment of the susceptibility of the terrain to erosion and classification into different susceptibility zones is an important step to understanding an area's vulnerability to erosion for development of proper management plans and mitigation strategies (Dai and Lee 2002; Ayalew et al. 2004; Bijukchhen et al. 2013; Erener et al. 2016; Pham et al. 2017). Susceptibility mapping is generally used in landslide and gully erosion modelling, the goal of which is to identify potentially vulnerable areas which are those with several critical variables. To understand the susceptibility of a region to erosion, either as landslides or gullying, different methods which use expert opinion (qualitative), statistical prediction (quantitative), or both may be applied using geographical information systems (GIS).

In order to assess the susceptibility, a number of geo-environmental variables such as geomorphology, slope, land use, lithology, etc., as well as palaeo locations of the phenomena have been used (Kheir et al. 2007; Akgün and Türk 2011; Dewitte et al. 2015; Kavzoglu et al. 2014; Gómez-Gutiérrez et al. 2015; Chen et al. 2016a; Garosi et al. 2018). Among these, most of the parameters considered as natural parameters and the land use/land cover existed in the area is only man made i.e. it was mainly controlled human activity. Expert opinion method relies on the field knowledge and expertise of the analyst to determine the influence and weights of each parameter and parameter classes, whereas statistical techniques use well defined bivariate or multivariate analysis techniques through dependent and independent variables to determine the relative importance of each variable (Bourenane et al. 2015; Rahmati et al. 2016). The suitability and selection of methods to produce susceptibility map is often heavily depend on the availability of data sets of independent geo-environmental variables particularly information on previous incidents of landslides or gullies (Lucà et al. 2011; Conoscenti et al. 2013; Park et al. 2013; Shit et al. 2015; Althuwaynee et al. 2016; Rahmati et al. 2017; Torri et al. 2018; Othman et al. 2018). Although the output of susceptibility analysis may vary in name such as landslide susceptibility zonation (LSZ) map or gully erosion susceptibility map, the analysis techniques and geo-environmental variables used in the modelling are generally similar. Further details of different techniques used to analyse terrain erosion susceptibility can be found in Aleotti and Chowdhury (1999), Guzzetti et al. (1999), van Westen (2000), Brenning (2005), Huabin et al. (2005), and van Westen et al. (2006).

In the present study, an attempt has been made to model and classify the upper catchment regions of the Baram River (Sarawak, Malaysia) in terms of susceptibility of the terrain to erosion due to gullying, soil slip, and landslides. The region considered possesses very weak geological formations (tightly folded sedimentary rocks of various lithologies) covered by dense forest. During the last few decades, the study area has undergone intense terrain modification and forest clearing through timber harvesting and logging road construction which increased the vulnerability of the terrain to erosion (Fig. 1). As a result of episodes of heavy rainfall, areas with high vulnerability to erosion will flow or slide downhill to valley streams and may deposit large quantities of sediment in the rivers downstream. Very few studies have reported on terrain susceptibility to erosion in Sarawak and the reported studies deal with the soil erosion assessment using soil loss equations (USLE /RUSLE) (Besler 1987; de Neergaard et al. 2008; Vijith et al. 2018a, 2018b; Vijith and Dodge-Wan 2018). Prior to 2018, no studies were reported from the selected upper catchment region of the Baram River.

The present study is an initial attempt to assess terrain erosion susceptibility and can be used as a basic and valuable information while planning for roads and other infrastructure developments. The study area lacks a database of previous information related to erosion (gullying and landslides in particular) and due to the relatively inaccessible nature of the terrain, it is difficult to map the locations of slides or gullies by direct observation in the field. To overcome these limitations, a well-defined and tested predictive analysis model, i.e. the analytical hierarchy process (AHP) which uses a combination of expert opinion and statistical measurements, was applied in this research. Numerous researchers have used the analytical hierarchy process to estimate the susceptibility to landslide or soil erosion in other parts of the world and found it to be successful in predicting the vulnerability of the region based on the parameters used (Komac 2006; Neaupane and Piantanakulchai 2006; Yoshimatsu and Abe 2006; Yalcin 2008; Nekhay et al. 2009; Svoray et al. 2012; Reis et al. 2012; Kayastha et al.

Fig. 1 Slope failures observed in the study area

2013; Pourghasemi et al. 2012, 2013a; Youssef 2015; Althuwaynee et al. 2016; Sangchini et al. 2016; Rahaman and Aruchamy 2017; Arabameri et al. 2018b). The findings of the present research will facilitate the identification of areas critically vulnerable to erosion and landslides and thus provides an opportunity to avoid risk associated with terrain susceptibility while implementing the developmental schemes in the region.

Study area

A forested region in the interior Sarawak, which has undergone vegetation changes and terrain alteration due to logging activities was selected for the present analysis. The study area covers a total area of 2105 km^2 and contains two major subwatersheds of the Baram River namely Sungai Patah and Sungai Akah which are located between north latitudes 3° 13′ 15″ to 3° 41′ 50″ and east longitudes 114° 35′ 42″ to 115° 13′ 20″ (Fig. 2). Though the subwatersheds differ in shape, both have similar terrain and geological characteristics. The area is highly undulating with elevations between 37 m to 1578 m asl. The bed rock consists of sedimentary rocks of Paleocene, Oligocene, and Miocene ages. Most of the study area consists of Oligocene shale and sandstone, with areas of Paleocene deep water sediments composed of shale and sandstone with occasional conglomerate and limestone, and Miocene shale and sandstone. Numerous anticlines, synclines, and local fractures are present in the area showing tight folds with a common northeast (NE) - southwest (SW) to north northeast (NNE) - south southwest (SSW) trend. The drainage pattern is predominantly dendritic but the presence of trellis and parallel pattern in the region indicates the influence of lithology and structural features on the development of drainage networks. Geomorphological features vary from highly elevated steep sloping escarpments to low lying flat regions of fluvial floodplains. Hills and mounds show highly complex shapes with a sharp crests to rounded tops. The area receives an annual average rainfall of approximately 4600 mm from the two dominant monsoon seasons viz., southwest and northeast monsoons. Rainfall shows high spatial and temporal variations (Vijith and Dodge-Wan 2018) Vegetation cover varies from dense primary forest to open spaces of barren land. The majority of the study area is covered with forests of different types and density, followed by mixed agricultural land (mainly hill paddy cultivation) and then the open spaces with no vegetation related to road development, villages, and logging. Initial field observations indicated that the development of logging roads and log trail (skidding and pulling trails) have rendered the terrain more susceptible to erosion by changing the continuity of the hills through toe cutting and removal of the protective vegetation cover.

Materials and methods

The Sungai Akah and Sungai Patah catchments of the Baram River were selected for the present research as

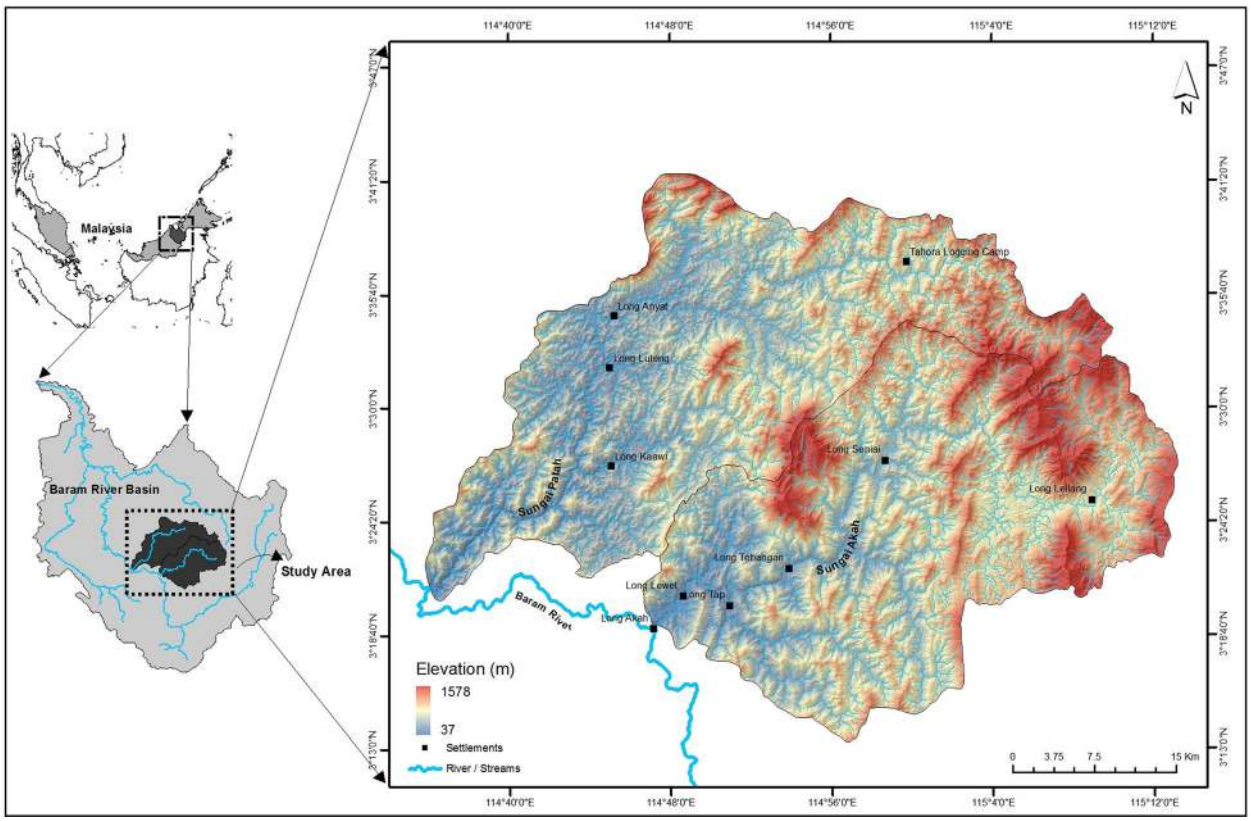

Fig. 2 Study area location map

this is a data poor region. Mapping of terrain erosion susceptibility is considered as the preliminary step to understand the risks of soil erosion and landslide. An erosion susceptibility map was generated using several geo-environmental variables derived from various remote sensing data sources such as digital elevation model (DEM) and satellite images. The digital elevation model, downloaded from the earth explorer (http://earthexplorer.usgs.gov) website of U. S Geological Survey. Shuttle Radar Topographic Mission (SRTM) data of 30 m was used after it had been clipped to the study area boundary and the voids filled by the Fill DEM module available in the spatial analyst extension of ArcGIS software. The filled elevation dataset was then used to derive variables such as slope, aspect, relative relief, slope length and steepness (LS) factor, curvature, landforms, topographic wetness index (TWI), and stream power index (SPI). Stream networks were produced from the digital elevation model and stream head points were extracted to calculate the stream head density map. The parameters are natural features of the region and terrain and not affected by anthropogenic activities. Landsat 8 OLI images of the area acquired on 28th March 2015, which reflect the current land use pattern were used to produce the land use/land cover map through supervised classification with field verification. Land use/land cover is the most significant factor under the influence of anthropogenic activities which modify the protective vegetation cover. Different software used for the generation of variables and final analysis are ArcGIS version 9.3 and SAGA version 2.1, which operates in the raster GIS environment and the cell size for this analysis was fixed as 30 × 30 m. The significance and methodology applied to obtain each variable is described in text, as well as the weightages attributed to each class of each variable.

In order to generate the terrain susceptibility map of the study area by analyzing the contribution of each variable which makes the terrain susceptible to erosion, the analytical hierarchy process (AHP) technique developed by Saaty (1980) was used. This methods has the capability of integrating expert knowledge, field information, and relative statistics together. AHP is a semi-quantitative, multi-criteria decision support technique which is used to generate high quality and precise decisions through the application of the matrix based pairwise comparison of the contributing factors which determine the results of the phenomenon or the process (Saaty 1990; Saaty 1994; Saaty and Vargas 2001). The pairwise comparison will be carried out based on the different ratings of each variable or feature classes on

the basis of relative importance varying from 1 to 9. Each value in the relative importance can be assigned to variable or variable classes based on the subjective judgement of relative importance. Relative weight of the variables used in the matrices can be determined by generations of eigenvectors and the consistency of the variable can be assessed by calculating the consistency index (CI) as given below (Saaty 1990) (Eq. 1):

$$CI = \frac{(\lambda max\text{-}n)}{(n\text{-}1)} \quad (1)$$

where, λ_{max} is the largest or principal eigenvalue of the analysed matrix and n is the order of the square matrix.

This inconsistency index can also be expressed as consistency ratio (CR) which determine the suitability of individual parameters and their classes to be included in the analysis and was given by the Eq. (2):

$$CR = \frac{CI}{RI} \quad (2)$$

where, RI is the random index i.e. consistency index for a random square matrix of the same size proposed by Saaty (1980). The cut-off of the CR was fixed as less than or equal to 0.1 so that if CR of the analyzed variable is found to be higher than the cut-off, the variable will be omitted from the analysis.

Preparation of terrain Erosion susceptibility zonation (TESZ) map

In order to map the areas susceptible to terrain erosion and classify them based on the severity and criticality of risk, a number of distinct geo-environmental variables were considered. The combined effects of multiple variables in terrain susceptibility were characterised through the application of analytical hierarchy process (AHP) based influence measuring technique, which is considered a powerful and supportive multiple criteria decision making tool (Malczewski 1999; Yasser et al. 2013; Chen et al. 2016b). Ten individual factors were used. They are: slope, aspect, relative relief, LS factor, curvature, landforms, TWI, SPI, stream head density, and land use/land cover (Fig. 3a-j). The contribution of each parameter in the terrain susceptibility as a single unit and individual feature classes in the parameters were determined by the cross comparison matrices analysed through the AHP and output rating was considered as the weight of each parameter and their class. Table 1 shows the pairwise comparison matrix, consistency ratio, and the weightings of individual parameters, and their classes considered in the analysis.

In all analysis which deals with terrain susceptibility, the primary factor considered is the terrain slope, which represents the inclination of the topography with reference to horizontal. Nature of the slope varies from gentle to steep and this controls different geomorphic processes such as erosion, transportation, and deposition in relation to the rainfall-runoff characteristics of the region (Foumelis et al. 2004; Gómez-Gutiérrez et al. 2015; Sangchini et al. 2016; Arabameri et al. 2018a). Gentle slopes are expected to induce less terrain slips due to low shear stresses (Lee et al. 2004). High slope values show the highest susceptibility to erosion although vertical terrain surfaces, and very high slopes having exposed bedrock show less susceptibility to terrain erosion due to less or nil soil cover (Dewitte et al. 2015; Rahmati et al. 2017; Torri et al. 2018). In order to generate the slope, hydrologically corrected (void filled) SRTM DEM were used and the slope map generated shown a range varies from 0 to 75°. Then the slope was reclassified into the following gentle to very critical seven classes 0–5°, 5°-10°, 10°-15°, 15°-25°, 25°-35°, 35°-45°, and > 45° and the relative percentage of area covered by individual slope class shown high spatial variation. Among the slope classes, a large percentage of the study area falls within the slope class 15°-25° (31%), followed by 10°-15° (20%), and 25°-35° (17%). It was also observed that, the higher slope classes in the range of 35–45° and > 45° occupied comparatively reduced areas of 9% and 1% only respectively. Seven slope classes were ranked by attributing factor scores from 1 to 9 to generate the pairwise matrix. The attribution was based on the assumption that there is a regular increase in risk across all the slope classes. Considering the influence of the slope over the terrain stability, relative weightages were then calculated and these vary from 0.0274 to 0.2432 (Table 1). Higher ratings are noted in areas having a slope higher than 35^0 in the study area.

Slope aspect indicates the direction of the terrain slope with respect to north and varies from − 1 to 359°, in which the negative value represents flat surface (Prasannakumar et al. 2011). Aspect of the terrain have direct and indirect control over terrain processes and conditions such as soil moisture, vegetation cover, and soil thickness by exposing the surface to sunlight and or heavy rain (Clerici et al. 2006; Meten et al. 2015). In most of the landslide and gully erosion modelling studies, slope aspects is taken as an important variable (Reis et al. 2012; Pourghasemi et al. 2013b; Rahmati et al. 2016; Sangchini et al. 2016; Menggenang and Samanta 2017; Othman et al. 2018). In the present research, a slope aspect map was generated from the elevation surface and classified into nine classes which are: flat, N, NE, E, SE, S, SW, W, and NW based on the orientation i.e. which way the terrain is facing. Considering the area distribution of the individual aspect class in the study area, most of the slope aspects classes cover similar areas (13%) except flat terrain which is very rare (0.30%).

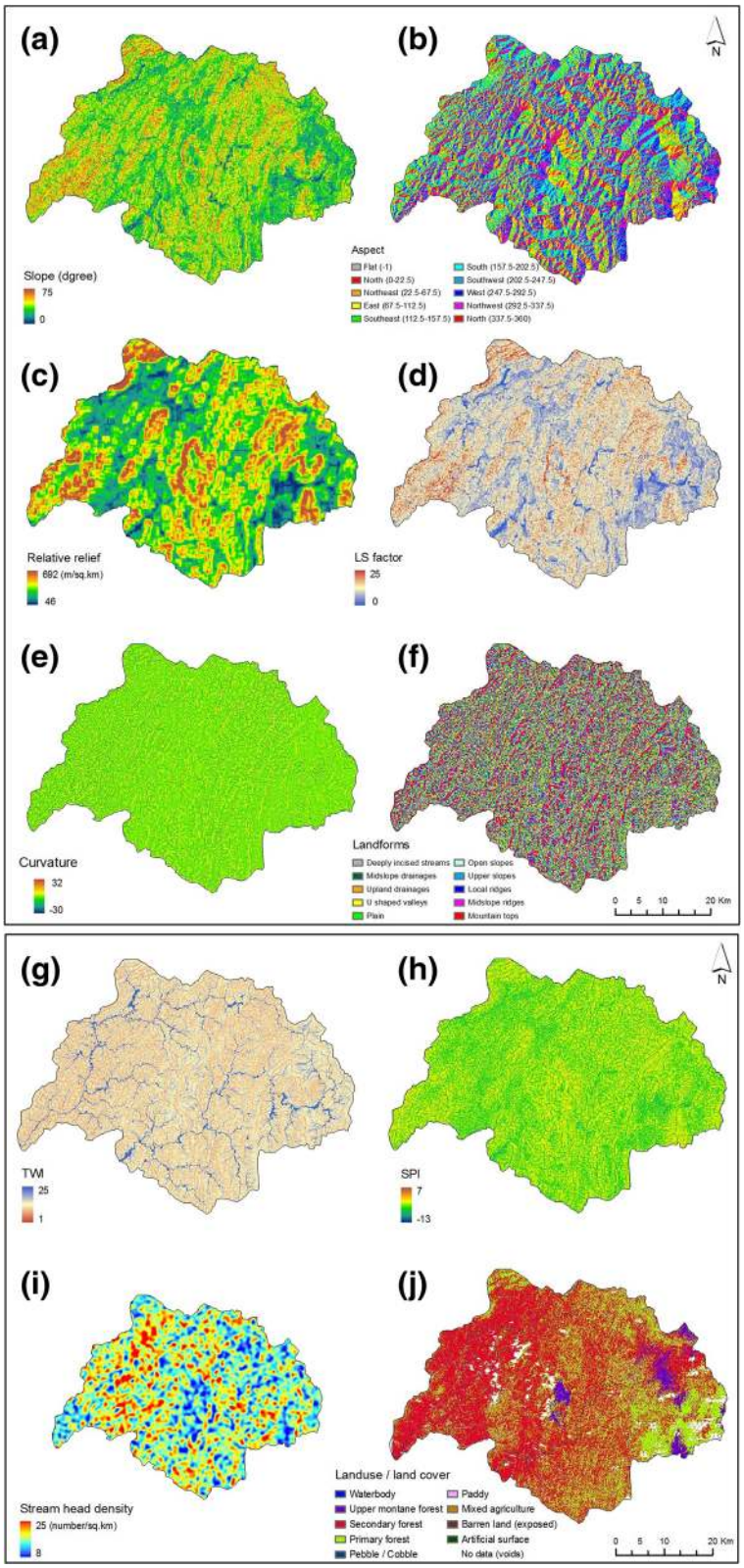

Fig. 3 Geo-environmental variables used in the analysis **a** Slope **b** Aspect **c** Relative relief **d** Slope length and steepness (LS) **e** Curvature **f** Landforms **g** topographic wetness index (TWI) **h** Stream power index (SPI) **i** Stream head density **j** Land use/land cover

Table 1 Pair-wise comparison matrix, ratings, and consistency ratio of the variables classes and individual variables used in the present study

Variables	Classes	1	2	3	4	5	6	7	8	9	10	Rating / weights
Slope	0–5	1	1/3	1/4	1/5	1/7	1/8	1/9				0.0270
	5–10		1	3/4	3/5	3/7	3/8	3/9				0.0810
	10–15			1	4/5	4/7	4/8	4/9				0.1081
	15–25				1	5/7	5/8	5/9				0.1351
	25–35					1	7/8	7/9				0.1891
	35–45						1	8/9				0.2162
	> 45							1				0.2432
Aspect	Flat	1	1/2	1/2	1/3	1/4	1/5	1/7	1/9	1/6		0.0256
	N		1	1	2/3	2/4	2/5	2/7	2/9	2/6		0.0512
	NE			1	2/3	2/4	2/5	2/7	2/9	2/6		0.0512
	E				1	3/4	3/5	3/7	3/9	3/6		0.0769
	SE					1	4/5	4/7	4/9	4/6		0.1025
	S						1	5/7	5/9	5/6		0.1282
	SW							1	7/9	7/6		0.1794
	W								1	9/6		0.2307
	NW									1		0.1538
Relative relief	< 100	1	1/3	1/5	1/7	1/9						0.04
	100–200		1	3/5	3/7	3/9						0.12
	200–300			1	5/7	5/9						0.2
	300–400				1	7/9						0.28
	> 400					1						0.36
Slope length and Steepness (LS)	5	1	1/3	1/7	1/9							0.05
	10		1	3/7	3/9							0.15
	15			1	7/9							0.35
	> 15				1							0.45
Curvature	Concave	1	9	9/7								0.5294
	Flat		1	1/7								0.0588
	Convex			1								0.4117
Landforms	Deeply incised stream	1	2/4	2/9	2/1	2/6	2/3	2/5	2/2	2/3	2/7	0.0476
	Midslope drainages		1	4/9	4/1	4/6	4/3	4/5	4/2	4/3	4/7	0.0952
	Upland drainages			1	9	9/6	9/3	9/5	9/2	9/3	9/7	0.2142
	U shaped valleys				1	1/6	1/3	1/5	1/2	1/3	1/7	0.0238
	Plains					1	6/3	6/5	6/2	6/3	6/7	0.1428
	Open slopes						1	3/5	3/2	3/3	3/7	0.0714
	Upper slopes							1	5/2	5/3	5/7	0.1190
	Local ridges								1	2/3	2/7	0.0476
	Midslope ridges									1	3/7	0.0714
	Mountain tops										1	0.1666
Topographic wetness index (TWI)	Low (< 5)	1	1/4	1/9								0.0714
	Moderate(5–10)		1	4/9								0.2857
	High (> 10)			1								0.6428
Stream power index (SPI)	< 0	1	1/2	1/3	1/4	1/6	1/8	1/9				0.0303
	0–1		1	2/3	2/4	2/6	2/8	2/9				0.0606

Table 1 Pair-wise comparison matrix, ratings, and consistency ratio of the variables classes and individual variables used in the present study *(Continued)*

Variables	Classes	1	2	3	4	5	6	7	8	9	10	Rating / weights
	1–2			1	3/4	3/6	3/8	3/9				0.0909
	2–3				1	4/6	3/8	4/9				0.1212
	3–4					1	6/8	6/9				0.1818
	4–5						1	8/9				0.2424
	> 5							1				0.2727
Stream head density	Low (< 15)	1	1/4	1/9								0.0714
	Medium (15–20)		1	4/9								0.2857
	High > 20			1								0.6428
Land use/land cover (LULC)	Water	1	1/1	1/8	1/2	1/1	1/2	1/9	1/9	1/1		0.0294
	Upper montane forest		1	1/8	1/2	1/1	1/2	1/9	1/9	1/1		0.0294
	Secondary forest			1	8/2	8/1	8/2	8/9	8/9	8/1		0.2359
	Primary forest				1	2/1	2/2	2/9	2/9	2/1		0.0588
	Pebble cobble					1	1/2	1/9	1/9	1/1		0.0294
	Paddy						1	2/6	2/9	2/1		0.0588
	Mixed agriculture							1	9/9	9/1		0.2647
	Exposed soil (barren)								1	9/1		0.2647
	Artificial surface									1		0.0294
Consistency ratio (CR): < 0.0001												
Variables(as single unit)	Slope	1	8/1	8/4	8/5	8/3	8/2	8/4	8/7	8/6	8/9	0.1633
	Aspect		1	1/4	1/5	1/3	1/2	1/4	1/7	1/6	1/9	0.0204
	Relative Relief			1	4/5	4/3	4/2	4/4	4/7	4/6	4/9	0.0816
	Slope length and steepness				1	5/3	5/2	5/4	5/7	5/6	5/9	0.1020
	Curvature					1	3/2	3/4	3/7	3/6	3/9	0.0612
	Landform						1	2/4	2/7	2/6	2/9	0.0408
	TWI							1	4/7	4/6	4/9	0.0816
	SPI								1	7/6	7/9	0.1429
	Stream head density									1	6/9	0.1224
	LULC										1	0.1837
Consistency ratio (CR): < 0.00003												

NE facing slopes were also below average (10.70%). Before applying the relative weightages to individual aspect class, slope instability observed during the field visit was considered. During the field visit, it was noted that, west facing slopes in general as well as southwest and northwest show more incidence of slope failure and gully erosion than any others. Therefore, while attributing the factor scores to generate the pairwise matrix, higher scores were given to slopes facing west, southwest, and northwest directions and relative weightages or ratings were calculated which vary in the range of 0.0256 to 0.2307.

Another important parameter which controls the terrain stability is the change in elevation in the unit area which is termed as relative relief. Terrains with higher relative relief indicates higher runoff and less infiltration and shows higher susceptibility to erosion (Raja et al. 2017). The relative relief of the study area was generated from the digital elevation model using the neighborhood range function available in the spatial analyst extension of ArcGIS software by keeping the unit size of the area as 1 km^2. The relative relief calculated for the study area ranges from 46 m/km^2 to 692 m/km^2 and was then divided into five classes which are: < 100 m/km^2, 100–200 m/km^2, 200–300 m/km^2, 300–400 m/km^2 and, > 400 m/km^2. Considering the area distribution of individual classes of relative relief in the selected study area, the majority (95%) falls within the three classes from 100 to 400 m/km^2. Within this 95%, more than 43% of the total area has relative relief in the range of 200–300 m/km^2 followed by 30% of the total area with relative relief in the range of 100–200 m/km^2 and 22% of the area in the range of 300–400 m/km^2. It was noted that very low and very high relative relief zones

($< 100\ m/km^2$ and $> 400\ m/km^2$) cover significantly less areas of 1% and 4% respectively only. Review of previous works carried out in landslide and gully erosion modelling which used the theme relative relief as a parameter indicates higher potentiality of areas with high relative relief in conditioning for erosion (Foumelis et al. 2004; Zhu et al. 2014; Pourghasemi et al. 2013a; Sangchini et al. 2016). Based on this prior and proven information, in the present research while attributing the factor scores to generate the pairwise matrix, higher scores were given to relative relief class having higher values and lower scores were assigned to low relative relief class. The relative weightages thus calculated varied from 0.040 to 0.36.

LS factor corresponds to the combined effect of slope length and its steepness, which have direct bearing on the erosion and the transportation potential of an area (Pourghasemi et al. 2013b; Vijith and Dodge-Wan 2018). An area with high slope and elongated nature has high potential for generating runoff and this directly influences the development of rills in the terrain in response to heavy rainfall (Haan et al. 1994; Panagos et al. 2015; Correa-Muñoz and Higidio-Castro 2017). Therefore, in the present analysis the LS factor was considered and generated from the digital elevation model through the methodology proposed by Moore and Burch (1986a, 1986b) using SAGA 2.1. The generated LS factor value varies from 0 to 25 and was divided into four classes which are: < 5, 5–10, 10–15, and > 15 considering its contribution to erosion susceptibility. Within the study area of Sungai Patah and Sungai Akah watersheds, 50% of the terrain has low LS values (< 5) and 41% has LS value between 5 and 10. Only 9% of the area has LS value of 10–15 and only 1% has LS value over 15. Soil and gully erosion modelling conducted by researchers in various locations identified the role of higher LS factor in initiating erosion and transportation of material from a region downstream (Nekhay et al. 2009; Pourghasemi et al. 2012; Shit et al. 2015; Arabameri et al. 2018a). Based on this in the present research also, while assigning the factor scores, more importance were given to classes showing high LS factor values and relative weightages were calculated which vary in the range of 0.05 to 0.45.

The topographic curvature used in the analysis represents the shape of the slope or topography which has direct bearing on the erosion by either concentrating runoff or dispersing it (Lee and Sambath 2006; Fischer et al. 2012). Topographic curvature may show an upward convex surface (positive curvature) or upwardly concave surface (negative curvature), or it may be flat (zero curvature) (Alkhasawneh et al. 2013). In order to understand the influence of the shape of the surface slope over terrain susceptibility, curvature was generated from the DEM. Topographic curvature in the study area ranges from − 30 to + 32, i.e. from concave surfaces to flat and convex surfaces. In the study area, the topography consists of both concave and convex curvature surfaces which together cover 94% of total area whereas flat areas only cover 6%. This is due to the complex and highly undulating nature of folded sedimentary rocks within the study area. Considering the shape of the land surface, both concave and convex surfaces possess susceptibility to erosion. But in the study area, during the field visits, it was noted that compared to convex surface the more gullies are observed in a concave surfaces. Further, while considering the previous studies reported from other parts of the world, most studies marked concave surfaces as more vulnerable to gullying and erosion (Pourghasemi et al. 2012; Meten et al. 2015; Youssef 2015; Raja et al. 2017). Therefore, while assigning the factor scores, more importance was given to concave curvature than convex by attributing higher scores and the calculated ratings are 0.0588 (flat), 0.4117 (convex), and 0.5294 (concave).

In order to produce a reliable terrain erosion susceptibility map, the specific landforms present in the study area needs to be included in the analysis. Landforms controls many spatial topographic erosional and depositional processes and was an integral part of geomorphometry (Seif 2014). Surface runoff, soil moisture distribution, vegetation characteristic, and even the water quality are influenced by the specific landforms (Mokarram et al. 2015). Therefore in the present research, the topographic position index based landform classification proposed by Weiss (2001) was selected to generate the landforms using digital elevation model. Topographic position index analysis identified ten landforms in the Sungai Akah and Patah area. They are deeply incised streams, midslope drainages, upland drainages, U-shaped valleys, plains, open slopes, upper slopes, local ridges, midslope ridges, and mountain tops. Within the study area, 39% of the total area is covered by deeply incised streams whereas mountain tops cover 30%. Besides these, local ridges (12%), upland drainages (10%), U-shaped valleys (4%), and upper slopes (3%) are also present. The remaining three landform classes (midslope drainages, open slopes, midslope ridges, and plains) cover less 1% of the total area only. Later, by considering the relative importance of individual landforms over the terrain susceptibility to erosion as explained in the previous studies conducted to model the landside susceptibility in various regions (Costanzo et al. 2012; Tien Bui et al. 2012; Oh and Lee 2017), factor scores were fixed and ratings were calculated. Calculated ratings vary from 0.0142 (Plain) to 0.2142 (Upland drainages).

The parameters discussed above all contribute to a certain extent to increase the susceptibility of the terrain to erosion. In addition, the contribution of water flow in

the terrain to enhance the susceptibility was also considered by means of topographic wetness index (TWI), derived from the digital elevation model. TWI considers the upslope contributing area and its slope to quantify the steady state wetness and water flow across the region (Pourghasemi et al. 2013a). TWI generated for the study area shows values in the range of 1 to 25 which have been divided into three classes which are: < 5, 5–10, and > 10. Considering the wetness potential of the area through TWI classes, 30% of the total study area was found to have low wetness index (TWI < 5) whereas most of the area (62% of the total area) shown moderate wetness index (5–10), while remaining 8% of the area has high TWI values (> 10). To take into account different level of contribution of TWI to terrain erosion susceptibility, landslide, and gully erosion susceptibility studies carried out in different locations were considered (Wang et al. 2015; Chen et al. 2017; Arabameri et al. 2018b). It was noted that, in most studies high TWI has high impact on erosion and in the present study, the relative scores of individual TWI classes were assigned based on the TWI values i.e. lower score were attributed to low TWI and vice versa. The calculated weightages varies from 0.0714 (TWI < 5) to 0.6428 (TWI > 10).

Another parameter is stream power index (SPI), which estimates the capacity of streams to potentially modify the geomorphology of an area through gully erosion and transportation. SPI is the measure of the erosive power of flowing water by considering the relationship between discharge and specific catchment area (Chen and Yu 2011; Pourghasemi et al. 2013b). SPI highlights areas in which overland flow has higher erosive power in the catchment (Wilson and Gallant 2000). This makes the use of SPI a significant parameter of interest in erosion and terrain susceptibility modelling. SPI was calculated for the study area using the stream power index module available in SAGA 2.1 software based on the digital elevation model as input data. SPI of the Baram study area varies from − 13 to 7 indicating the differential erosive power of the streams in the region. Higher values indicate the likely overland flow paths during storms or severe erosive rainfall pointing to potential areas for gullying or other areas susceptible of erosion. The SPI map prepared was reclassified into seven classes which are: < 0, 0–1, 1–2, 2–3, 3–4, 4–5, and > 5. Most of the study area (63%) showed SPI value less than 0. High SPI represent areas where high slopes and flow accumulations exist which indicate enhanced with erosive potential (Gómez-Gutiérrez et al. 2015; Arabameri et al. 2018a). Considering the SPI values and their contribution towards terrain susceptibility and gullying, the relative scores were added to each class in a simple progression and rating was calculated and the rating varies in the range of 0.0303 to 0.2727.

Another parameter of interest is stream head density which indicates the number of stream origin points per the unit area. Analysis of channel head locations can provide insight into the controls on drainage density as well as the response of landscapes to climatic change and indication about the rate of susceptibility of that terrain (Wadge 1988; Montgomery and Dietrich 1989; Lin and Oguchi 2004). In the present study, the stream head density was calculated by extracting the starting points of all 1st order streams in the study area. Using the density function available in the spatial analyst extension of ArcGIS, stream head density was calculated for 1 km^2 and the calculated density values were found to vary from 8 to 25 N/km^2. Reclassification of stream head density in to three classes which are: low (< 15 N/km^2), medium (15–20 N/km^2), and high (> 20 N/km^2) was then used for the calculation of individual weights. It was noted that, 21% of the total study area has low stream head density whereas 71% of the area has moderate density, and remaining 7% of the area only has high density. Areas having high stream head density is more susceptible to erosion, especially by the development of gully head and continuous erosion downstream. Based on the density classes and its impact on terrain erosion susceptibility, the relative scores of the stream head density classes were assigned. Further, ratings were calculated and it varies in the range of 0.0714 to 0.6428 indicating varying contribution towards the terrain susceptibility.

In erosion susceptibility analysis, the existing land use/land cover of the area under consideration also plays a vital role by providing information about the condition of vegetative protection against erosion and many researchers found land use/land cover to be a dominant variable in erosion susceptibly (Dai and Lee 2002; Glade 2003; Beguería 2006; Leh et al. 2013; Galve et al. 2015; Mandal and Mandal 2018; Vuillez et al. 2018; Abdulkareem et al. 2019). It is also one of the key factors under anthropogenic influence i.e. reflective of human disturbance of vegetation cover due to logging, clearing for roads, and/or agriculture. In the present study, the land use/land cover map of the area was derived from Landsat 8 OLI images acquired on 28th March 2015, through the supervised classification with extensive ground truth points from field observations. The segmentation of Landsat image into classified land use/land cover map has identified and mapped the following land use/land cover classes in the area: water, secondary forest, primary forest, montane forest, mixed agriculture, paddy, exposed soil (barren), artificial surfaces, and pebbles, cobbles in river beds. The supervised classification indicate that more than 56% of the total area was covered by secondary forests and 27% of the area was covered by primary forests. It was also noted that, land use activities like mixed agricultural land and exposed barren land, which alter the terrain condition

in the region, cover 8.8 and 1.8% of the total area respectively. The other land use/land cover classes together cover less than 5.5% of the total area, in which upper montane forests cover 3.35% of the area. Further, when determining the relative influence of individual land use/land cover classes in terrain susceptibility, previous study which detail the influence of individual land use classes in soil erosion vulnerability of the area was taken into account (Vijith and Dodge-Wan 2018). For the AHP, the weight was calculated for individual land use/land cover classes based on the relative importance assigned to each class and varied in the range of 0.0294 to 0.2647. Among the different classes, the exposed barren land, mixed agriculture acquired the highest rating of 0.2647 followed by secondary forest (0.2352) whereas the upper montane forest and artificial surface showed the lowest weight (0.0294). Higher weight shown by the exposed barren land, mixed agriculture, and secondary forest in soil erosion study (Vijith et al. 2018a, 2018b) indicates the strong influence of these land use classes on terrain susceptibility.

In order to produce the terrain erosion susceptibility zonation (TESZ) map, the ranking of individual parameters was carried out to assign their relative contribution before assigning the calculated weight to each parameter classes. The parameter ranking indicated that land use/land cover is the highest influencing parameter with a rating of 0.183 followed by slope (0.163), stream power index (0.142), and stream head density (0.122). The other parameters such as aspect, relative relief, LS factor, curvature, landforms, and topographic wetness index were found to have less influence. Reliability of each parameter to be included in the analysis was determined by examining the consistency ratio (CR) and it was noted that all the parameters shown CR below the proposed cut-off of 0.1, so none were omitted from the analysis. Finally, the weights calculated for individual parameter classes were assigned to the respective parameters to produce the weighted maps and using the raster calculator option of the spatial analyst, individual themes were integrated to produce the terrain erosion susceptibility index (TESI) map using the equation (Eq. 3):

$$\begin{aligned}\text{Terrain erosion susceptibility index (TESI)} = {} & {}_{wt}\text{Slope} * 0.163 + {}_{wt}\text{Aspect} * 0.020 \\ & + {}_{wt}\text{Relative relief} * 0.081 + {}_{wt}\text{LS factor} * 0.102 \\ & + {}_{wt}\text{Curvature} * 0.061 + {}_{wt}\text{Land forms} * 0.040 \\ & + {}_{wt}\text{TWI} * 0.081 + {}_{wt}\text{SPI} * 0.142 \\ & + {}_{wt}\text{Stream head density} * 0.122 \\ & + {}_{wt}\text{Land use/land cover} * 0.183 \end{aligned} \quad (3)$$

where, $_{wt}$ is the relative weights of classes in individual variable.

Result and discussion

Ten geo-environmental variables which are potentially responsible for changing the stability of the terrain rendering it more susceptible to erosion were considered quantitatively to assess the susceptibility of the forested region of Sarawak to erosion using the AHP technique. Among the ten variables used to generate the terrain erosion susceptibility index (TESI) map, the variables such as land use/land cover, slope, stream power index, stream head density, and slope length and steepness factors shown maximum influence (> 0.10) followed the relative relief and topographic wetness index (0.08). Other variables such as curvature (0.06) and landform (0.04) shown moderate influence, whereas aspect was found to be the lowest influencing variable with a rank of 0.02. Even though, the variable ranks differ, the selection of the variables in the present analysis are found to be optimum by showing the CR less than the cut-off value (0.00003). Besides this, the weight factor calculated for the individual variable classes indicates a varying degree of influences within the parameter and between the parameters. It was also noted that the relative weighting of variable classes indicates the variability of influences. Among the variables considered, the land use/land cover, terrain with slope > 25° having west, southwest, and northwest orientations, relative relief > 300 m/km^2; high LS factor, and concavity, having high TWI, upland drainages and mountain top landforms, high stream head density are showing high relative weights among the classes and contributing more to the terrain susceptibility. The integration of weighted variables in the raster calculator resulted terrain erosion susceptibility index (TESI) map showing the susceptibility ranges from 0.07 to 0.34 indicating spatial distribution of different degree of susceptibility to erosion (Fig. 4a). The TESI map generated shows varying distribution of higher and lower susceptibility indexes all over the area without showing any particular pattern, which make it difficult to identify and differentiate the regions which showing nil or low susceptibility and very high susceptibility.

In order to understand the spatial extent of different severity of erosion susceptibility, the TESI map was reclassified into five discrete classes based on the susceptibility index values namely nil, low, moderate, high, and very high zones (Fig. 4b). The reclassification of the TESI to terrain erosion susceptibility zonation (TESZ) map facilitated the calculation of areal extent of different susceptibility zones. The areas falling under each erosion susceptibility class are given in Table 2 and shown in Fig. 5. The final TESZM showed that 10.3% of the study area is categorised as having very high susceptibility to erosion and these areas appears to be distributed different places in the region. In addition, high erosion susceptibility zones occupy 14.9% whereas moderate and

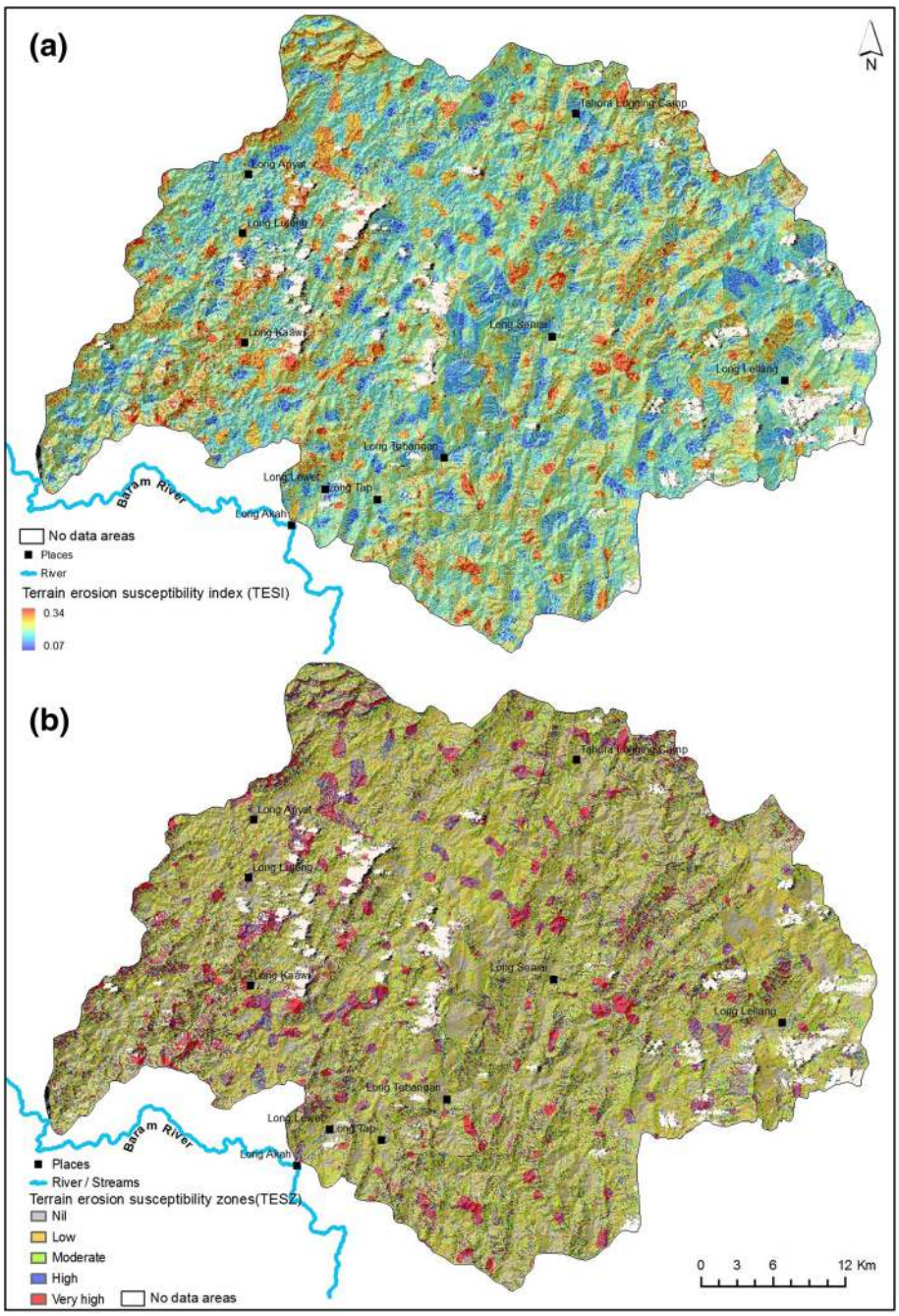

Fig. 4 **a** Terrain erosion susceptibility index (TESI) maps and **b** Classified terrain erosion susceptibility zonation (TESZ) map

low susceptibility zones covers 25.8 and 27.1% of the area respectively. It was also noted that 17.47% of the study area is not prone to erosion. Besides this, 4% of the area was not included in the final analysis as there is no data in these zones due to thick cloud and cloud shadow on satellite image. An attempt has been made to understand the spatial characteristics of the erosion susceptibility zones by overlying the TESZ with the exaggerated terrain model. It was found that the higher erosion susceptibility zones mostly occur in the flanks of the mountains rather than in the valleys. In addition, in some places these zones show linear patterns which can be linked directly with the road structure and skidder trails. For the development of roads in the area, the continuity of hills with concave or convex slopes has been removed by the toe cutting and this will increase the susceptibility to erosion and lead to the development of soil slumps triggered by the heavy rainfall. The clustered

Table 2 Terrain erosion susceptibility classes derived from the reclassification of TESI

Terrain erosion susceptibility classes	Area (km^2)	Area (%)	Probability of terrain erosion
Nil	367.84	17.47	No chance of erosion, mostly low lying areas.
Low	572.01	27.17	Very low probability. Mostly affected by the run-off from the higher elevation
Moderate	544.77	25.88	Medium probability, may directly involve in erosion or affected as part of falling from the top
High	313.22	14.88	High certainty of erosion either as slide or gullying. Need attention in such areas crossing road sections.
Very High	217.31	10.32	Very high certainty of erosion either as slide or gullying. To be monitored during the heavy rainy seasons.
No data	89.85	4.27	No data is available due to cloud and shadow in the image. Not considered in the analysis

nature of the higher erosion susceptibility indicates the logging activity and shifting cultivation, which exposes the terrain by removing the protective tree cover.

Rainfall distribution

Though different geo-environmental variables make the terrain susceptible to erosion, the amount and intensity of rainfall which falls in an area acts as the triggering mechanism which can initiate movement of soil, debris, and other overburden downstream. In most studies, rainfall distribution is included as a theme to statistically model the land susceptibility to erosion (Sangchini et al. 2016). In the present research, rainfall distribution in the study area was considered separately and analysed to identify the areas with high possibility of terrain erosion susceptibility. Therefore, 5 year rainfall data were collected from the Department of Irrigation and Drainage (DID) Malaysia corresponding to four rain gauges located in the study area and six around the area. Mean monthly rainfall distribution and 5 year mean monthly, and annual rainfall is shown in Fig. 6. It was noted that mean monthly rainfall varies between 238 mm (June) to 532 mm (November) with long term mean monthly and annual rainfall of 352 mm 4227 mm respectively. A spatial distribution map was generated by considering the mean annual rainfall calculated for each rain gauge for use in further analysis (Fig. 7). Mean rainfall ranges between 3654 to 4862 mm with higher rainfall generally located in southwest part of the study area, especially between the rain gauges Long Naha'ah and Long Akah whereas comparatively lower rainfall is noted in northern and north-eastern part of the study area.

In order to assess the contribution of rainfall to terrain susceptibility leading to slope failure, 200 random (unconditional and unstratified) points (pixel size 30 × 30 m) were generated within the study area boundary and mean annual rainfall, TESI, and TESZ values corresponding to each point were extracted. The extracted values of TESI and TESZ were compared by linear regression with mean annual rainfall to study the possible

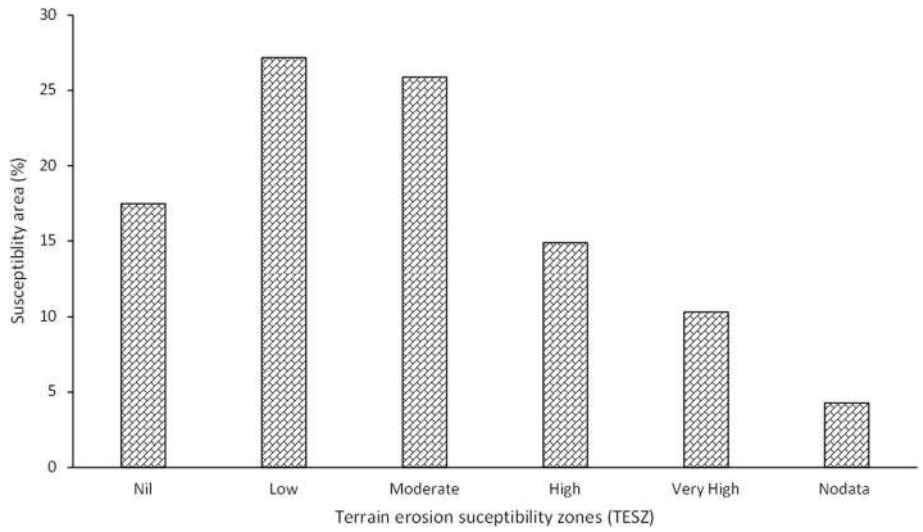

Fig. 5 Area distribution of terrain erosion susceptibility zones

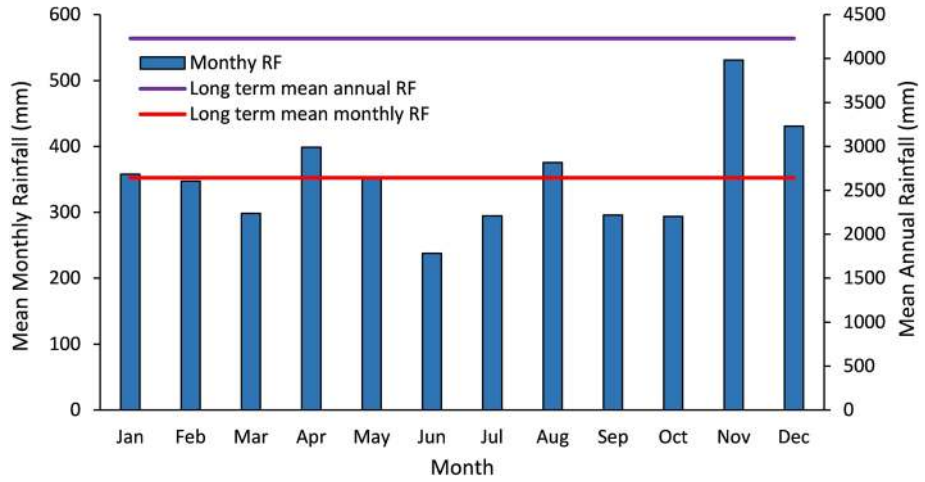

Fig. 6 Mean monthly and annual rainfall distribution in the study area

role of local rainfall amount and distribution over terrain susceptibility (Lyra et al. 2014; Teodoro et al. 2016; Brito et al. 2017) (Fig. 8). Linear regression plot of mean annual rainfall and TESI indicates very low or nil correlation (Fig. 8a). Similarly, the linear regression plot of the mean annual rainfall distribution and TESZ shows absence of correlation (Fig. 8b). *P* values ($p > 0.10$) also indicates no or nil dependency between the dependant (terrain susceptibility) and independent (rainfall) variables in the region. Although high rainfall in general is a

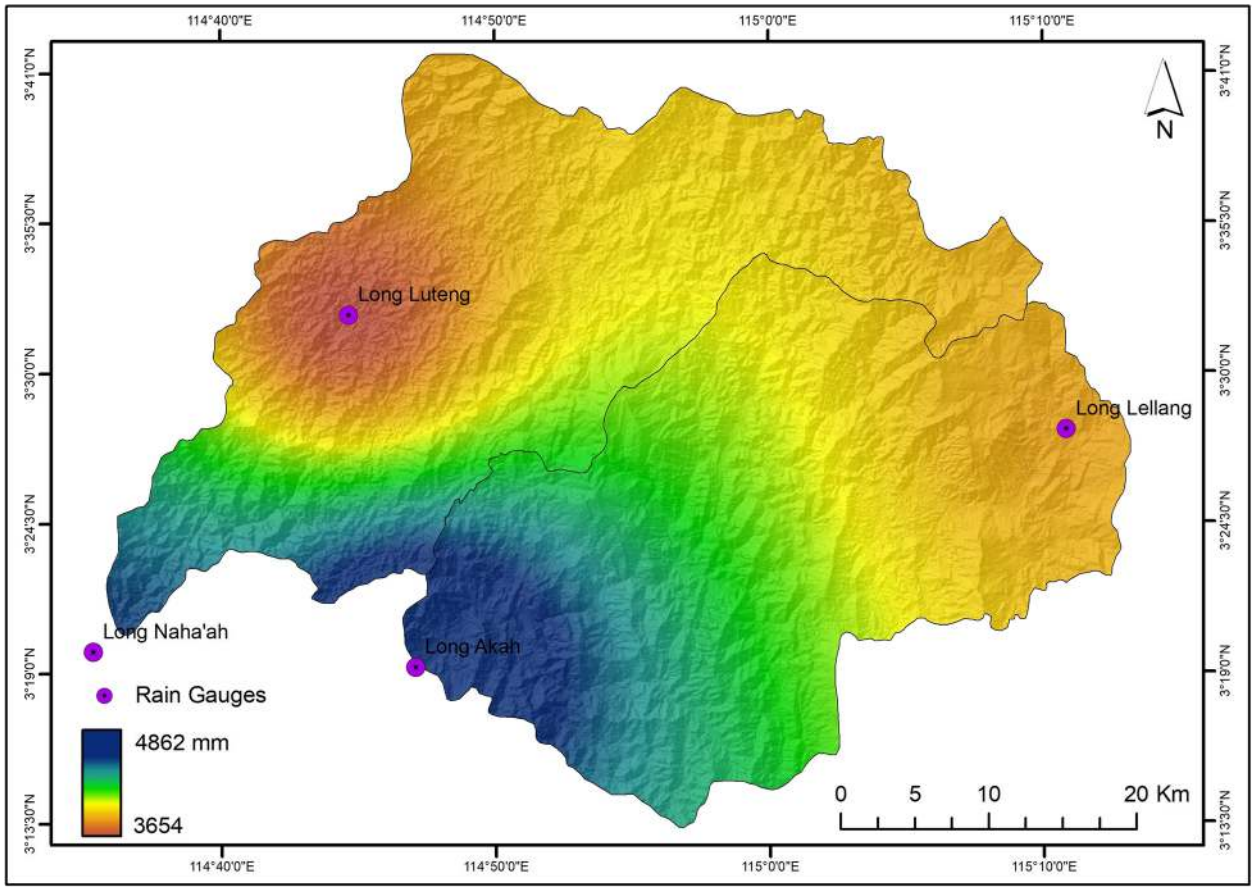

Fig. 7 Spatial distribution of mean annual rainfall in the study area

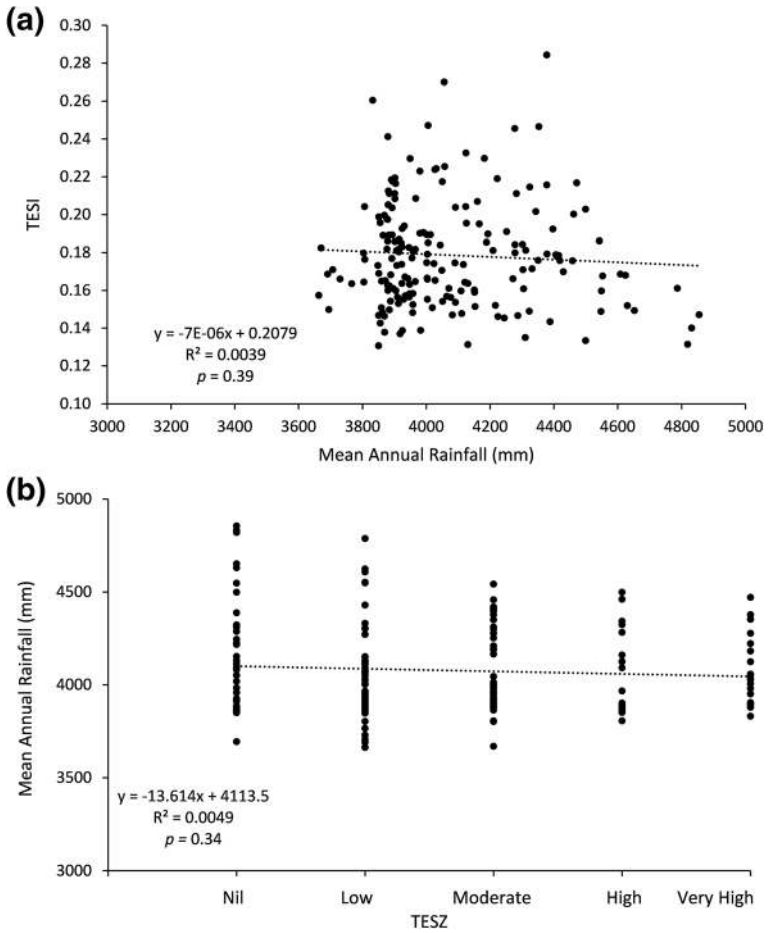

Fig. 8 Linear regression plots explaining the relationship between rainfall **a** TESI and **b** TESZ

factor in increasing terrain erosion susceptibility, at a specific local scale (pixel size 30 × 30 m area), the higher amount of rainfall received in parts of the region does not appear to significantly influence the local site specific terrain susceptibility. However, other geo-environmental variables considered play more significant roles in rendering the terrain more susceptible to erosion in specific local areas.

Conclusion

The characteristic probability of erosion proneness of a sample catchment with regenerated and logged tropical rain forest region in Sarawak, northern Borneo, was successfully carried out in the present study using raster GIS and AHP technique. Terrain variables derived from the digital elevation model such as slope, aspect, relative relief, LS factor, curvature, landforms, TWI, SPI, stream head density, and the land use/land cover interpreted from the satellite images were integrated in the raster based GIS environment after deriving the determinant ranking and weights for the variables and variable classes. The generation of rankings and weightages for the variables considered in the analysis through the AHP technique facilitated the identification of the most crucial variables which render the terrain more susceptible to erosion. Though all these variables were found to be contributing to erosion susceptibility to various degrees, the determination of ranks through relative ratio highlights that land use/land cover, slope, stream power index, stream head density, and LS factor are the most crucial variables. In the study area, the places which are exposed (barren land) with concave slopes having slope exceeding 25° and facing west, southwest, and northwest, with relative relief higher than 300 m/km^2 and high LS factor, TWI and stream head density are found to be the most vulnerable to erosion. These areas are identified via the TESI and TESZ maps.

TESZ map generated by the reclassification of TESI into five distinct groups show the spatial pattern of erosion susceptibility in terms of its severity. It was found that 10 and 14% of the total area comes under the very high and high erosion susceptibility zones. The higher susceptibility was found to be characteristic of high elevated hills and slopes which undergo rapid changes.

However, areas with nil and low potential of erosion susceptibility together constitute 44% and the moderate susceptibility zones occupy 25% of the total study area. Considering the influence of rainfall in the region, the entire study area receives what can be considered high tropical rainfall. Analysis of 200 randomly distributed pixel sized area (30 m × 30 m) suggests that at local scale rainfall is not strongly correlated with erosion susceptibility. The field observations and the erosion susceptibility map indicates that the root causes of the terrain susceptibility are modification of land use and the development of logging roads, and skidder trails. Barren areas reduce the stability of the terrain and particularly when combined with other factors such as slope, LS factor. Along with this, the high amount of rainfall recorded throughout the region induces movement of unsupported and toe-cut slopes to move downstream. The findings of the present study give a better understanding of the region in terms of erosional characteristics. The findings can be used for planning of new roads, settlements by developing and implementing erosion reduction and terrain protection measures.

Abbreviations

AHP: Analytical Hierarchy Process; CI: Consistency Index; GIS: Geographical Information Systems; LS factor: Slope Length and Steepness factor; LSZ: Landslide Susceptibility Zonation; RUSLE: Revised Universal Soil Loss Equation; SPI: Stream Power Index; SRTM: Shuttle Radar Topographic Mission; TESI: Terrain Erosion Susceptibility Index; TESZ: Terrain Erosion Susceptibility Zonation; TWI: Topographic Wetness Index; USLE: Universal Soil Loss Equation

Acknowledgements

The authors wish to thank Sarawak Energy Berhad for funding this research under the Project "Mapping of Soil Erosion Risk". They also thank Curtin University Malaysia for facilities and other assistance and the Department of Irrigation and Drainage (DID), Malaysia for providing rainfall data. Authors are also thankful to the Editor in Chief, and anonymous reviewers for their critical reviews, constructive comments, and suggestions which significantly improved the quality of the manuscript.

Authors' contributions

VH done technical, scientific analysis of the research and developed the manuscript. DDW read and suggested few amendments in the analysis and structure of the manuscript and also reviewed the final manuscript, including language correction. All authors read and approved the final manuscript.

Funding

This research was carried out as part of the project "Mapping of Soil Erosion Risk" funded by Sarawak Energy Berhad (RD01/2014(C)), Malaysia.

Availability of data and materials

Not applicable.

Competing interests

The authors declare that they have no competing interests.

Received: 26 February 2019 Accepted: 21 June 2019
Published online: 12 July 2019

References

Abdulkareem, J.H., B. Pradhan, W.N.A. Sulaiman, and N.R. Jamil. 2019. Prediction of spatial soil loss impacted by long-term land-use/land-cover change in a tropical watershed. *Geoscience Frontiers* 10 (2): 389–403.

Akgün, A., and N. Türk. 2011. Mapping erosion susceptibility by a multivariate statistical method: A case study from the Ayvalık region, NW Turkey. *Computers & Geosciences* 37 (9): 1515–1524.

Aleotti, P., and R. Chowdhury. 1999. Landslide hazard assessment: Summary review and new perspectives. *Bulletin of Engineering Geology and the Environment.* 58: 21–44.

Alkhasawneh, M.S., U.K. Ngah, L.T. Tay, M. Isa, N. Ashidi, and M.S. Al-batah. 2013. Determination of important topographic factors for landslide mapping analysis using MLP network. *The Scientific World Journal.* https://doi.org/10.1155/2013/415023.

Althuwaynee, O.F., B. Pradhan, and S. Lee. 2016. A novel integrated model for assessing landslide susceptibility mapping using CHAID and AHP pair-wise comparison. *International Journal of Remote Sensing.* 37 (5): 1190–1209.

Arabameri, A., B. Pradhan, H.R. Pourghasemi, K. Rezaei, and N. Kerle. 2018a. Spatial modelling of gully Erosion using GIS and R programing: A comparison among three data mining algorithms. *Applied Sciences.* 8 (8): 1369.

Arabameri, A., K. Rezaei, H.R. Pourghasemi, S. Lee, and M. Yamani. 2018b. GIS-based gully erosion susceptibility mapping: A comparison among three data-driven models and AHP knowledge-based technique. *Environmental Earth Sciences.* 77 (17): 628.

Ayalew, L., H. Yamagishi, and N. Ugawa. 2004. Landslide susceptibility mapping using GIS-based weighted linear combination, the case in Tsugawa area of Agano River, Niigata prefecture, Japan. *Landslides* 1 (1): 73–81.

Beguería, S. 2006. Changes in land cover and shallow landslide activity: A case study in the Spanish Pyrenees. *Geomorphology.* 74 (1–4): 196–206.

Besler, H. 1987. Slope properties, slope processes and soil erosion risk in the tropical rain forest of Kalimantan Timur (Indonesian Borneo). *Earth surface Processes and landforms* 12 (2): 195–204.

Bijukchhen, S.M., P. Kayastha, and M.R. Dhital. 2013. A comparative evaluation of heuristic and bivariate statistical modelling for landslide susceptibility mappings in Ghurmi–Dhad Khola, East Nepal. *Arabian Journal of Geosciences* 6 (8): 2727–2743.

Bourenane, H., Y. Bouhadad, M.S. Guettouche, and M. Braham. 2015. GIS-based landslide susceptibility zonation using bivariate statistical and expert approaches in the city of Constantine (Northeast Algeria). *Bulletin of Engineering Geology and the Environment* 74 (2): 337–355.

Brenning, A. 2005. Spatial prediction models for landslide hazards: Review, comparison and evaluation. *Natural Hazards and Earth System Science* 5: 853–862.

Brito, T.T., J.F. Oliveira-Júnior, G.B. Lyra, G. Gois, and M. Zeri. 2017. Multivariate analysis applied to monthly rainfall over Rio de Janeiro state, Brazil. *Meteorology and Atmospheric Physics* 129 (5): 469–478.

Chen, C.Y., and F.C. Yu. 2011. Morphometric analysis of debris flows and their source areas using GIS. *Geomorphology.* 129 (3–4): 387–397.

Chen, W., H. Chai, X. Sun, Q. Wang, X. Ding, and H. Hong. 2016a. A GIS-based comparative study of frequency ratio, statistical index and weights-of-evidence models in landslide susceptibility mapping. *Arabian Journal of Geosciences.* 9 (3): 204.

Chen, W., W. Li, H. Chai, E. Hou, X. Li, and X. Ding. 2016b. GIS-based landslide susceptibility mapping using analytical hierarchy process (AHP) and certainty factor (CF) models for the Baozhong region of Baoji city, China. *Environmental Earth Sciences* 75 (1): 1–14.

Chen, W., X. Xie, J. Wang, B. Pradhan, H. Hong, D.T. Bui, Z. Duan, and J. Ma. 2017. A comparative study of logistic model tree, random forest, and classification and regression tree models for spatial prediction of landslide susceptibility. *Catena.* 151: 147–160.

Clerici, A., S. Perego, C. Tellini, and P. Vescovi. 2006. A GIS-based automated procedure for landslide susceptibility mapping by the conditional analysis method: The Baganza valley case study (Italian northern Apennines). *Environmental Geology* 50 (7): 941–961.

Conoscenti, C., V. Agnesi, S. Angileri, C. Cappadonia, E. Rotigliano, and M. Märker. 2013. A GIS-based approach for gully erosion susceptibility modelling: A test in Sicily, Italy. *Environmental Earth Sciences* 70 (3): 1179–1195.

Correa-Muñoz, N.A., and J.F. Higidio-Castro. 2017. Determination of landslide susceptibility in linear infrastructure. Case: Aqueduct network in Palacé, Popayan (Colombia). *Ingeniería e Invest.* 37 (2): 17–24.

Costanzo, D., E. Rotigliano, C. Irigaray Fernández, J.D. Jiménez-Perálvarez, and J. Chacón Montero. 2012. Factors selection in landslide susceptibility modelling on large scale following the GIS matrix method: Application to the river Beiro basin (Spain). *Natural Hazards and Earth System Sciences.* 12: 327–340.

Dai, F.C., and C.F. Lee. 2002. Landslide characteristics and slope instability modeling using GIS, Lantau Island, Hong Kong. *Geomorphology* 42 (3–4): 213–228.

de Neergaard, A., J. Magid, and O. Mertz. 2008. Soil erosion from shifting cultivation and other smallholder land use in Sarawak, Malaysia. *Agriculture, Ecosystems & Environment.* 125 (1): 182–190.

Dewitte, O., M. Daoudi, C. Bosco, and M. Van Den Eeckhaut. 2015. Predicting the susceptibility to gully initiation in data-poor regions. *Geomorphology.* 228: 101–115.

Erener, A., A. Mutlu, and H.S. Düzgün. 2016. A comparative study for landslide susceptibility mapping using GIS-based multi-criteria decision analysis (MCDA), logistic regression (LR) and association rule mining (ARM). *Engineering Geology* 203: 45–55.

Fadul, H.M., A.A. Salih, A.A. Imad-eldin, and S. Inanaga. 1999. Use of remote sensing to map gully erosion along the Atbara River, Sudan. *International Journal of Applied Earth Observation and Geoinformation* 1 (3): 175–180.

Fischer, J.T., J. Kowalski, and S.P. Pudasaini. 2012. Topographic curvature effects in applied avalanche modeling. *Cold Regions Science and Technology* 74: 21–30.

Foumelis, M., E. Lekkas, and I. Parcharidis. 2004. Landslide susceptibility mapping by GIS-based qualitative weighting procedure in Corinth area. *Bulletin of the Geological Society of Greece* 36 (2): 904–912.

Galve, J.P., A. Cevasco, P. Brandolini, and M. Soldati. 2015. Assessment of shallow landslide risk mitigation measures based on land use planning through probabilistic modelling. *Landslides.* 12 (1): 101–114.

Garosi, Y., M. Sheklabadi, H.R. Pourghasemi, A.A. Besalatpour, C. Conoscenti, and K. Van Oost. 2018. Comparison of differences in resolution and sources of controlling factors for gully erosion susceptibility mapping. *Geoderma.* 330: 65–78.

Glade, T. 2003. Landslide occurrence as a response to land use change: A review of evidence from New Zealand. *Catena.* 51 (3–4): 297–314.

Gómez-Gutiérrez, Á., C. Conoscenti, S.E. Angileri, E. Rotigliano, and S. Schnabel. 2015. Using topographical attributes to evaluate gully erosion proneness (susceptibility) in two Mediterranean basins: Advantages and limitations. *Natural Hazards.* 79 (1): 291–314.

Guzzetti, F., A. Carrara, M. Cardinali, and P. Reichenbach. 1999. Landslide hazard evaluation: A review of current techniques and their application in a multi-scale study, Central Italy. *Geomorphology* 31: 81–216.

Haan, C.T., B.J. Barfield, and J.C. Hayes. 1994. *Design hydrology and sedimentology for small catchments*. San Diego: Elsevier.

Huabin, W., L. Gangjun, X. Weiya, and W. Gonghui. 2005. GIS based landslide hazard assessment: An overview. *Progress in Physical Geography.* 29 (4): 548–567.

Kavzoglu, T., E.K. Sahin, and I. Colkesen. 2014. Landslide susceptibility mapping using GIS-based multi-criteria decision analysis, support vector machines, and logistic regression. *Landslides.* 11 (3): 425–439.

Kayastha, P., M.R. Dhital, and F. De Smedt. 2013. Application of the analytical hierarchy process (AHP) for landslide susceptibility mapping: A case study from the Tinau watershed, West Nepal. *Computers & Geosciences.* 52: 398–408.

Kheir, R.B., J. Wilson, and Y. Deng. 2007. Use of terrain variables for mapping gully erosion susceptibility in Lebanon. *Earth Surface Processes and Landforms.* 32 (12): 1770–1782.

Komac, M. 2006. A landslide susceptibility model using the analytical hierarchy process method and multivariate statistics in perialpine Slovenia. *Geomorphology.* 74 (1): 17–28.

Lee, S., J.H. Ryu, J.S. Won, and H.J. Park. 2004. Determination and application of the weights for landslide susceptibility mapping using an artificial neural network. *Engineering Geology* 71 (3–4): 289–302.

Lee, S., and T. Sambath. 2006. Landslide susceptibility mapping in the Damrei Romel area, Cambodia using frequency ratio and logistic regression models. *Environmental Geology* 50 (6): 847–855.

Leh, M., S. Bajwa, and I. Chaubey. 2013. Impact of land use change on erosion risk: An integrated remote sensing, geographic information system and modeling methodology. *Land Degradation & Development.* 24 (5): 409–421.

Lin, Z., and T. Oguchi. 2004. Drainage density, slope angle, and relative basin position in Japanese bare lands from high-resolution DEMs. *Geomorphology.* 63 (3–4): 159–173.

Lucà, F., M. Conforti, and G. Robustelli. 2011. Comparison of GIS-based gullying susceptibility mapping using bivariate and multivariate statistics: Northern Calabria, South Italy. *Geomorphology* 134 (3): 297–308.

Lyra, G.B., J.F. Oliveira-Júnior, and M. Zeri. 2014. Cluster analysis applied to the spatial and temporal variability of monthly rainfall in Alagoas state, northeast of Brazil. *International Journal of Climatology* 34 (13): 3546–3558.

Malczewski, J. 1999. *GIS and multi-criteria decision analysis*. 1st ed, 392. New York: Wiley.

Mandal, S., and K. Mandal. 2018. Modeling and mapping landslide susceptibility zones using GIS based multivariate binary logistic regression (LR) model in the Rorachu river basin of eastern Sikkim Himalaya, India. *Model Earth Systems and Environment* 4 (1): 69–88.

Menggenang, P., and S. Samanta. 2017. Modelling and mapping of landslide hazard using remote sensing and GIS techniques. *Model Earth Systems and Environment.* 3 (3): 1113–1122.

Meten, M., N. Prakash Bhandary, and R. Yatabe. 2015. Effect of landslide factor combinations on the prediction accuracy of landslide susceptibility maps in the Blue Nile gorge of Central Ethiopia. *Geoenvironmental Disasters.* 2 (1): 9.

Mokarram, M., G. Roshan, and S. Negahban. 2015. Landform classification using topography position index (case study: Salt dome of Korsia-Darab plain, Iran). *Model Earth Systems and Environment.* 1 (4): 40.

Montgomery, D.R., and W.E. Dietrich. 1989. Source areas, drainage density, and channel initiation. *Water Resources Research.* 25 (8): 1907–1918.

Moore, I.D., and G.J. Burch. 1986a. Physical basis of the length slope factor in the universal soil loss equation. *Soil Science Society of America Journal.* 50 (5): 1294–1298.

Moore, I.D., and G.J. Burch. 1986b. Modeling erosion and deposition. Topographic effects. *Transactions of the ASAE* 29 (6): 1624–1630.

Neaupane, K.M., and M. Piantanakulchai. 2006. Analytic network process model for landslide hazard zonation. *Engineering Geology* 85 (3): 281–294.

Nekhay, O., M. Arriaza, and L. Boerboom. 2009. Evaluation of soil erosion risk using analytic network process and GIS: A case study from Spanish mountain olive plantations. *Journal of Environmental Management.* 90 (10): 3091–3104.

Oh, H.J., and S. Lee. 2017. Shallow landslide susceptibility modeling using the data mining models artificial neural network and boosted tree. *Applied Sciences.* 7 (10): 1000.

Othman, A.A., R. Gloaguen, L. Andreani, and M. Rahnama. 2018. Improving landslide susceptibility mapping using morphometric features in the Mawat area, Kurdistan region, NE Iraq: Comparison of different statistical models. *Geomorphology.* 319: 147–160.

Panagos, P., P. Borrelli, and K. Meusburger. 2015. A new European slope length and steepness factor (LS-factor) for modeling soil erosion by water. *Geosciences.* 5 (2): 117–126.

Park, S., C. Choi, B. Kim, and J. Kim. 2013. Landslide susceptibility mapping using frequency ratio, analytic hierarchy process, logistic regression, and artificial neural network methods at the Inje area, Korea. *Environmental Earth Sciences* 68 (5): 1443–1464.

Pham, B.T., D.T. Bui, H.R. Pourghasemi, P. Indra, and M.B. Dholakia. 2017. Landslide susceptibility assessment in the Uttarakhand area (India) using GIS: A comparison study of prediction capability of naïve bayes, multilayer perceptron neural networks, and functional trees methods. *Theoretical and Applied Climatology* 128 (1–2): 255–273.

Pourghasemi, H., B. Pradhan, C. Gokceoglu, and K.D. Moezzi. 2013b. A comparative assessment of prediction capabilities of Dempster–Shafer and weights-of-evidence models in landslide susceptibility mapping using GIS. *Geomatics Natural Hazards and Risk.* 4 (2): 93–118.

Pourghasemi, H.R., H.R. Moradi, and S.F. Aghda. 2013a. Landslide susceptibility mapping by binary logistic regression, analytical hierarchy process, and statistical index models and assessment of their performances. *Natural Hazards* 69 (1): 749–779.

Pourghasemi, H.R., B. Pradhan, and C. Gokceoglu. 2012. Application of fuzzy logic and analytical hierarchy process (AHP) to landslide susceptibility mapping at Haraz watershed, Iran. *Natural Hazards* 63 (2): 965–996.

Prasannakumar, V., R. Shiny, N. Geetha, and H. Vijith. 2011. Applicability of SRTM data for landform characterisation and geomorphometry: A comparison with contour-derived parameters. *International Journal of Digital Earth.* 4 (5): 387–401.

Rahaman, S.A., and S. Aruchamy. 2017. Geoinformatics based landslide vulnerable zonation mapping using analytical hierarchy process (AHP), a study of Kallar river sub watershed, Kallar watershed, Bhavani basin, Tamil Nadu. *Model Earth Systems and Environment.* 3 (1): 41.

Rahmati, O., A. Haghizadeh, H.R. Pourghasemi, and F. Noormohamadi. 2016. Gully erosion susceptibility mapping: The role of GIS-based bivariate statistical models and their comparison. *Natural Hazards.* 82 (2): 1231–1258.

Rahmati, O., N. Tahmasebipour, A. Haghizadeh, H.R. Pourghasemi, and B. Feizizadeh. 2017. Evaluating the influence of geo-environmental factors on gully erosion in a semi-arid region of Iran: An integrated framework. *Science of the Total Environment.* 579: 913–927.

Raja, N.B., I. Çiçek, N. Türkoğlu, O. Aydin, and A. Kawasaki. 2017. Landslide susceptibility mapping of the Sera River basin using logistic regression model. *Natural Hazards.* 85 (3): 1323–1346.

Reis, S., A. Yalcin, M. Atasoy, R. Nisanci, T. Bayrak, M. Erduran, C. Sancar, and S. Ekercin. 2012. Remote sensing and GIS-based landslide susceptibility mapping using frequency ratio and analytical hierarchy methods in Rize province (NE Turkey). *Environmental Earth Sciences.* 66 (7): 2063–2073.

Saaty, T.L. 1980. *The analytical hierarchy process*, 350. New York: McGraw Hill.

Saaty, T.L. 1990. *The analytic hierarchy process: Planning, priority setting, resource allocation.* 1st ed, 502. Pittsburgh: RWS Publications.

Saaty, T.L. 1994. *Fundamentals of decision making and priority theory with analytic hierarchy process.* 1st ed, 527. Pittsburgh: RWS Publications.

Saaty, T.L., and L.G. Vargas. 2001. *Models, methods, concepts, and applications of the analytic hierarchy process*. 1st ed, 333. Boston: Kluwer Academic.

Sangchini, E.K., S.N. Emami, N. Tahmasebipour, H.R. Pourghasemi, S.A. Naghibi, S. A. Arami, and B. Pradhan. 2016. Assessment and comparison of combined bivariate and AHP models with logistic regression for landslide susceptibility mapping in the Chaharmahal-e-Bakhtiari Province, Iran. *Arab Journal of Geosciences* 9 (3): 1–15.

Seif, A. 2014. Using topography position index for landform classification (case study: Grain Mountain). *Bulletin of Environment, Pharmacology and Life Sciences* 3: 33–39.

Shit, P.K., R. Paira, G. Bhunia, and R. Maiti. 2015. Modeling of potential gully erosion hazard using geo-spatial technology at Garbheta block, West Bengal in India. *Model Earth Systems and Environment* 1 (2): 1–16.

Svoray, T., E. Michailov, A. Cohen, L. Rokah, and A. Sturm. 2012. Predicting gully initiation: Comparing data mining techniques, analytical hierarchy processes and the topographic threshold. *Earth Surface Processes and Landforms* 37 (6): 607–619.

Teodoro, P.E., J.F. de Oliveira-Júnior, E.R. Da Cunha, C.C. Correa, F.E. Torres, V.M. Bacani, G. Gois, and L.P. Ribeiro. 2016. Cluster analysis applied to the spatial and temporal variability of monthly rainfall in Mato Grosso do Sul state, Brazil. *Meteorology and Atmospheric Physics* 128 (2): 197–209.

Thornbury, W.D. 1969. *Principles of geomorphology*. 2nd ed. New York: Wiley.

Tien Bui, D., B. Pradhan, O. Lofman, and I. Revhaug. 2012. Landslide susceptibility assessment in Vietnam using support vector machines, decision tree, and Naive Bayes Models. *Mathematical problems in Engineering*. https://doi.org/10.1155/2012/974638.

Torri, D., J. Poesen, M. Rossi, V. Amici, D. Spennacchi, and C. Cremer. 2018. Gully head modelling: A Mediterranean badland case study. *Earth Surface Processes and Landforms.* 43 (12): 2547–2561.

Van Westen, C.J. 2000. The modelling of landslide hazards using GIS. *Surveys in Geophysics.* 21: 241–255.

Van Westen, C.J., T.W.J. Van Asch, and R. Soeters. 2006. Landslide hazard and risk zonation why is still so difficult? *Bulletin of Engineering geology and the Environment.* 65: 167–184.

Vijith, H., and D. Dodge-Wan. 2018. Spatio-temporal changes in rate of soil loss and erosion vulnerability of selected region in the tropical forests of Borneo during last three decades. *Earth Science Informatics.* 11 (2): 171–181.

Vijith, H., A. Hurmain, and D. Dodge-Wan. 2018b. Impacts of land use changes and land cover alteration on soil erosion rates and vulnerability of tropical mountain ranges in Borneo. *Remote Sensing Applications: Society and Environment.* 12: 57–69.

Vijith, H., L.W. Seling, and D. Dodge-Wan. 2018a. Estimation of soil loss and identification of erosion risk zones in a forested region in Sarawak, Malaysia, northern Borneo. *Environment, Development and Sustainability.* 20 (3): 1365–1384.

Vuillez, C., M. Tonini, K. Sudmeier-Rieux, S. Devkota, M.H. Derron, and M. Jaboyedoff. 2018. Land use changes, landslides and roads in the Phewa watershed, Western Nepal from 1979 to 2016. *Applied Geography* 94: 30–40.

Wadge, G. 1988. The potential of GIS modelling of gravity flows and slope instabilities. *International Journal of Geographical Information System.* 2 (2): 143–152.

Wang, Q., W. Li, W. Chen, and H. Bai. 2015. GIS-based assessment of landslide susceptibility using certainty factor and index of entropy models for the Qianyang County of Baoji city, China. *Journal of Earth System Science* 124 (7): 1399–1415.

Weiss, A. 2001. Topographic position and landforms analysis. *Geomorphology.* 21: 251–264.

Wilson, J.P., and J.C. Gallant. 2000. Digital terrain analysis. *Terrain Analysis: Principles and Applications.* 6 (12): 1–27.

Yalcin, A. 2008. GIS-based landslide susceptibility mapping using analytical hierarchy process and bivariate statistics in Ardesen (Turkey): Comparisons of results and confirmations. *Catena.* 72 (1): 1–12.

Yasser, M., K. Jahangir, and A. Mohmmad. 2013. Earth damsite selection using the analytic hierarchy process (AHP): A case study in the west of Iran. *Arabian Journal of Geoscience.* 6 (9): 3417–3426.

Yoshimatsu, H., and S. Abe. 2006. A review of landslide hazards in Japan and assessment of their susceptibility using an analytical hierarchic process (AHP) method. *Landslides.* 3 (2): 149–158.

Youssef, A.M. 2015. Landslide susceptibility delineation in the Ar-Rayth area, Jizan, Kingdom of Saudi Arabia, using analytical hierarchy process, frequency ratio, and logistic regression models. *Environmental Earth Sciences.* 73 (12): 8499–8518.

Zhu, A.X., R. Wang, J. Qiao, C.Z. Qin, Y. Chen, J. Liu, F. Du, Y. Lin, and T. Zhu. 2014. An expert knowledge-based approach to landslide susceptibility mapping using GIS and fuzzy logic. *Geomorphology.* 214: 128–138.

Publisher's Note